

# Generalized Boltzmann hierarchy for massive neutrinos in cosmology

Caio Bastos de Senna Nascimento

*Department of Physics & Astronomy, Stony Brook University, Stony Brook, NY 11794*

Boltzmann solvers are an important tool for the computation of cosmological observables in the linear regime. They involve solving the Boltzmann equation, followed by an integration in momentum space, to arrive at the desired fluid properties. This is a cumbersome, computationally expensive procedure. In this work we introduce the so-called generalized Boltzmann hierarchy (GBH) for massive neutrinos in cosmology, a simpler alternative to the usual Boltzmann hierarchy, where the momentum dependence is integrated out leaving us with a two-parameter infinite set of ordinary differential equations. Along with the usual expansion in multipoles, there is now also an expansion in higher velocity weight integrals of the distribution function. We show that the GBH produces the density contrast neutrino transfer function to a per mille level accuracy at both large and intermediate scales compared to the neutrino free-streaming scale. Furthermore, by introducing a switch to a viscous fluid approximation after horizon crossing, we show that the GBH can achieve over all scales the same accuracy as the standard CLASS approach in its default precision settings. The GBH is then a powerful tool to include neutrino anisotropies in the computation of cosmological observables in linear theory, with integration being simpler and potentially faster than standard methods.

## INTRODUCTION

Neutrino oscillation experiments have established that neutrinos are massive particles (at least two eigenstates), with a lower bound, in the sum of all neutrino masses, of  $\sum m_\nu \geq 0.06\text{eV}$ ,  $0.1\text{eV}$  for normal and inverted hierarchies, respectively [1, 2]. The large-scale structure of our universe gives a sensitive probe of neutrino masses [3, 4]. This allows us to use cosmological data to constraint the sum of neutrino mass eigenstates:  $\sum m_\nu \lesssim (0.1-0.3)\text{eV}$ , e.g. [5, 6], depending on the choice of used data sets. Current and future large-scale structure surveys [7–13] will be used to determine the mass scale of neutrinos [14, 15], but also to constraint beyond- $\Lambda\text{CDM}$  scenarios [16, 17]. It is then of paramount importance that cosmological observables, such as the matter power spectrum, can be computed to a sub-percent level accuracy, in both linear and non-linear scales.

The study of structure formation in the non-linear regime relies on N-body simulations [18, 19]. On the other hand, the linear theory is much simpler, and there are publicly available codes, such as the code for anisotropies in the microwave background (CAMB) [20] and the cosmic linear anisotropy solving system (CLASS) [22], that can be used to compute the observables. The implementation of neutrinos in the linear theory is somewhat cumbersome, since it involves solving a Boltzmann hierarchy of equations in momentum space. The reason for this can be traced back to the usual statement that the momentum dependence in the distribution function cannot be integrated out [23]. For this reason, fluid approximations have been developed in the past, and incorporated as an optional tool in the Boltzmann solvers [25, 29].

In this work we show that the momentum dependence in the distribution function can, in fact, be exactly integrated out, at the expense of introducing a new countable parameter  $n$ , along with the parameter  $l$  associated to

the multipole expansion, to the infinite system of ODE's that need to be solved to determine the dynamics, in  $k$  space ([24] being an example of this in the literature). This leads us to a novel two-parameter infinite set of equations that determine the evolution of non-cold dark matter (or  $\text{ncdm}$ , borrowing notation from CLASS [25]) perturbations in a flat universe: The generalized Boltzmann hierarchy (GBH). Along with the usual multipole expansion, there is now also an expansion in higher velocity weight integrals of the distribution function. The GBH is simpler than the usual approach, as implemented in Boltzmann solvers, because it does not require the numerical computation of momentum integrals, after solving the dynamical equations.

The paper is organized as follows: In I, we introduce the generalized Boltzmann hierarchy for  $\text{ncdm}$  perturbations, and compare it to the usual approach of evolving the distribution function in phase space. In II, we implement the equations numerically for an individual neutrino component of mass  $m_\nu = 0.1\text{eV}$ , and for the intermediate scale of  $k = 0.01\text{Mpc}^{-1}$ , obtaining per mille agreement with the Boltzmann solver CLASS in high precision settings, for all values of redshift. We also discuss the dependence of this framework on the neutrino mass  $m_\nu$  and scale  $k$ , and show that when switching to a fluid approximation on small scales, i.e. once a given mode becomes smaller than the free-streaming scale, we can produce neutrino transfer functions with the same accuracy as CLASS in its default precision settings. In III, we conclude and discuss our findings. In the appendix A, we give a detailed account of the truncation scheme for the GBH. Finally, in the appendix B we investigate the GBH in the simple case of  $l_{\text{max}} = 2$  and  $n_{\text{max}} = 0$ , i.e. a viscous fluid approximation (FA). We compare the truncation scheme developed for the GBH with the one employed in CLASS.

## I. GENERALIZED BOLTZMANN HIERARCHY

We start by introducing the additional expansion in higher velocity weight integrals of the distribution function, followed by a derivation of their associated dynamical equations. We will be considering scalar (linear) perturbations to a flat Friedmann-Robertson-Walker (FRW) universe, in the Newtonian gauge

$$ds^2 = a(\tau)^2[-(1 + 2\psi)d\tau^2 + (1 - 2\phi)d\vec{x}^2] \quad (1)$$

Conventions and notation follows [23]. Let us first define suitable generalized fluid properties, at the level of background

$$P_n = \rho\omega_n := \frac{4\pi}{3}a^{-4} \int_0^\infty dq q^2 f_0(q) \epsilon \left(\frac{q}{\epsilon}\right)^{2n} \quad \forall n \geq 0 \quad (2)$$

where  $f_0(q) = (2/(2\pi)^3)(1 + e^{\frac{q}{T_0}})^{-1}$  is the Fermi-Dirac distribution written in terms of  $\vec{q} = a\vec{p}$ , with  $\vec{p}$  the proper momentum, to account for the redshifting of temperature, i.e.  $T_\nu = T_0 a^{-1}$ , with  $T_0 \approx 1.95\text{K}$  the temperature of relic neutrinos today. Also  $\epsilon = \sqrt{q^2 + a^2 m^2} = aE$ , with  $E$  the proper energy of an individual particle. Then  $P_0 = (1/3)\rho$  is a third of the background energy density,  $P_1 = P$  is the pressure,  $P_2 \equiv \mathcal{P}$ , and in general  $P_{n+2} \equiv \mathcal{P}^{(n)}$ ,  $n \geq 0$  are higher velocity weight pressures. Similarly,  $\omega_0 = 1/3$ ,  $\omega_1 = \omega$  is the equation of state parameter, and  $\omega_{n+2}$ ,  $n \geq 0$  are higher velocity weight equation of state parameters.

Taking the derivative of Eq.(2) with respect to conformal time gives the following hierarchy of equations

$$\begin{aligned} \omega'_n &= -(2n+3)\mathcal{H}\omega_n + (2n-1)\mathcal{H}\omega_{n+1} \\ &\quad - \frac{\rho'}{\rho}\omega_n \quad \forall n \geq 0 \end{aligned} \quad (3)$$

where  $\mathcal{H} = a'/a$ , and  $'$  denotes derivative with respect to conformal time. Notice that  $q/\epsilon = v_\nu \sim T_\nu/m_\nu$  is the physical velocity of an individual neutrino particle, such that the additional factors of  $(q/\epsilon)^2$  in the integrals in Eq.(2) effectively shift the peak of the distribution function to higher particle velocities. In the relativistic regime, all particles travel at the speed of light, and one only needs to consider the  $n = 0$  equation. The same holds in the non-relativistic regime, where  $v_\nu^2$  corrections become negligible. During the transition, however, the higher velocity weight fluid properties need to be taken into account, in order to probe the whole spectrum of neutrino particle velocities.

Setting  $n = 0$  in Eq.(3) yields the familiar equation  $\rho' + 3\mathcal{H}(\rho + P) = 0$ . At this level, it is easier to simply determine the evolution of the distribution function, and then integrate Eq.(2) directly, than to approach the infinite set of Eqs. (3). This is because the background distribution function admits a simple, analytic solution (e.g. Fermi-Dirac distribution). However, this is no longer true when inhomogeneities are introduced.

In this case we have, along with the expansion in higher velocity weight integrals of the distribution function, parametrized by  $n$ , the usual expansion in multipoles, parametrized by  $l$ . To obtain it, split the distribution function as  $f = f_0(1 + \Psi)$ , and expand  $\Psi$  in a Legendre series

$$\Psi(\vec{k}, \hat{n}, q, \tau) = \sum_{l=0}^{\infty} (-i)^l (2l+1) \Psi_l(k, q, \tau) P_l(\hat{k} \cdot \hat{n}) \quad (4)$$

where we are already working in  $\vec{k}$  space (set  $\vec{\nabla} \rightarrow i\vec{k}$ ), and define  $\hat{n} = \vec{q}/q$ .

In terms of the multipole expansion in Eq.(4), the fluid properties directly sourcing the gravitational field, i.e. in the energy momentum tensor, are [23]

$$\delta\rho = \rho\delta = 4\pi a^{-4} \int_0^\infty dq q^2 f_0(q) \epsilon \Psi_0 \quad (5a)$$

$$\delta P = \frac{4\pi}{3} a^{-4} \int_0^\infty dq q^2 f_0(q) \epsilon \left(\frac{q}{\epsilon}\right)^2 \Psi_0 \quad (5b)$$

$$(\rho + P)\theta = 4\pi k a^{-4} \int_0^\infty dq q^2 f_0(q) q \Psi_1 \quad (5c)$$

$$(\rho + P)\sigma = \frac{8\pi}{3} a^{-4} \int_0^\infty dq q^2 f_0(q) \epsilon \left(\frac{q}{\epsilon}\right)^2 \Psi_2 \quad (5d)$$

We now wish to generalize this to higher multipoles, and also include higher velocity weight integrals of the distribution function, in analogy to Eq.(2), to make sure that the whole spectrum of particle velocities is being probed during the transition from the relativistic to non-relativistic regimes. The following is then a natural choice of dynamical variables:

$$\delta P_n = \rho\delta_n := \frac{4\pi}{3} a^{-4} \int_0^\infty dq q^2 f_0(q) \epsilon \left(\frac{q}{\epsilon}\right)^{2n} \Psi_0 \quad (6a)$$

$$(\rho + P)\theta_n := 4\pi k a^{-4} \int_0^\infty dq q^2 f_0(q) \epsilon \left(\frac{q}{\epsilon}\right)^{2n+1} \Psi_1 \quad (6b)$$

$$(\rho + P)f_{l,n} := 4\pi \frac{l!}{(2l-1)!!} a^{-4} \int_0^\infty dq q^2 f_0(q) \epsilon \left(\frac{q}{\epsilon}\right)^{2n+l} \Psi_l \quad (6c)$$

$$\forall l \geq 1$$

and  $n \geq 0$  everywhere. Notice that  $\delta_0 = \frac{1}{3}\delta$  is a third of the density contrast,  $\rho\delta_1 = \delta P$  is the perturbation to the pressure,  $\rho\delta_2 \equiv \delta\mathcal{P}$ , and  $\rho\delta_{n+2} \equiv \delta\mathcal{P}^{(n)}$ ,  $n \geq 0$  are the perturbations to the higher velocity weight pressures. Also  $\theta_0 = \theta$  is the divergence of the velocity,  $\theta_1 \equiv \Theta$  and  $\theta_{n+1} \equiv \Theta^{(n)}$ ,  $n \geq 0$  are its higher velocity weight counterparts. We also define  $f_{2,n} \equiv \sigma_n$ , the anisotropic shear stress, with a similar notation for its higher velocity weight integrals (i.e.  $\Sigma^{(n)}$ ), and set  $\theta_n \equiv k f_{1,n}$ , when it is convenient to do so. In order to derive a set of equations for the variables in Eq.(6), we need the time evolution of the multipoles. It follows from the substitution of Eq.(4)

into the Boltzmann equation, and reads [23]

$$\Psi'_0 = -\frac{qk}{\epsilon}\Psi_1 - \phi' \frac{d \ln f_0}{d \ln q} \quad (7a)$$

$$\Psi'_1 = \frac{qk}{3\epsilon}(\Psi_0 - 2\Psi_2) - \frac{\epsilon k}{3q}\psi \frac{d \ln f_0}{d \ln q} \quad (7b)$$

$$\Psi'_l = \frac{qk}{(2l+1)\epsilon}[l\Psi_{l-1} - (l+1)\Psi_{l+1}] \quad \forall l \geq 2 \quad (7c)$$

Now take the derivative of each expression in Eq.(6) with respect to conformal time, and use Eqs.(2), (3), (6) and (7) to arrive at

$$\delta'_n = -(2n-3w)\mathcal{H}\delta_n + (2n-1)\mathcal{H}\delta_{n+1} \quad (8a)$$

$$- \frac{1}{3}(1+w)\theta_n + [(2n+3)\omega_n - (2n-1)\omega_{n+1}]\phi'$$

$$\theta'_n = -\left[(2n+1-3w)\mathcal{H} + \frac{w'}{1+w}\right]\theta_n + 2n\mathcal{H}\theta_{n+1} \quad (8b)$$

$$+ \frac{1}{1+w}k^2\delta_{n+1} - k^2\sigma_n$$

$$+ \frac{1}{1+w}[(2n+3)\omega_n - (2n-1)\omega_{n+1}]k^2\psi$$

$$f'_{l,n} = -\left[(2n+l-3w)\mathcal{H} + \frac{w'}{1+w}\right]f_{l,n} \quad (8c)$$

$$+ (2n+l-1)\mathcal{H}f_{l,n+1} + \frac{l^2}{4l^2-1}kf_{l-1,n+1}$$

$$- kf_{l+1,n} \quad \forall l \geq 2$$

with  $n \geq 0$ . This is the generalized Boltzmann hierarchy (GBH) for a ncdm component. Setting  $n = 0$  in Eq.(8), one recovers the usual ncdm fluid equations (and up to  $l = 2$ , including only dynamical equations for the fluid properties that directly source the gravitational field)

$$\delta' = -(1+w)(\theta - 3\phi') - 3\mathcal{H}\left(\frac{\delta P}{\delta\rho} - w\right)\delta \quad (9a)$$

$$\theta' = -\left[(1-3w)\mathcal{H} + \frac{w'}{1+w}\right]\theta + \frac{\delta P/\delta\rho}{1+w}k^2\delta - k^2\sigma + k^2\psi \quad (9b)$$

$$\sigma' = -\left[(2-3w)\mathcal{H} + \frac{w'}{1+w}\right]\sigma + \mathcal{H}\Sigma + \frac{4}{15}\Theta - kf_3 \quad (9c)$$

As is well known, Eq.(9) involves variables, i.e.  $\delta P/\delta\rho$ ,  $\Sigma$ ,  $\Theta$  and  $kf_3$ , that need to be somehow approximated, in terms of the dynamical variables in the system, in order to close the equations. On the other hand, the two-parameter hierarchy of Eqs.(8) is closed as it is, and we have achieved our goal: To get rid of the momentum integrals altogether. Of course, any practical implementation of the GBH requires a good truncation scheme: A choice of a given number of multipoles,  $l_{\max} + 1$ , and higher velocity weight variables,  $n_{\max} + 1$ , to dynamically evolve, together with a recipe for approximating higher order quantities. The resulting system of equations is of dimension  $(l_{\max} + 1) \times (n_{\max} + 1)$ . We discuss this at length in the appendix A. Here we will just spell out the

recipe. The truncation in multipoles is done with the approximation

$$f_{l_{\max}+1,n} \approx (l_{\max}+1) \left( \frac{1}{k\tau} f_{l_{\max},n} - \frac{l_{\max}}{4l_{\max}^2-1} f_{l_{\max}-1,n+1} \right) \quad (10)$$

while the truncation in higher velocity weight integrals is handled with

$$\frac{\delta_{n_{\max}+1}}{\delta_{n_{\max}}} \approx \frac{2n_{\max}+5}{2n_{\max}+3} \frac{\omega_{n_{\max}+1}}{\omega_{n_{\max}}} \frac{1 - \frac{2n_{\max}+1}{2n_{\max}+5} \frac{\omega_{n_{\max}+2}}{\omega_{n_{\max}+1}}}{1 - \frac{2n_{\max}-1}{2n_{\max}+3} \frac{\omega_{n_{\max}+1}}{\omega_{n_{\max}}}} \quad (11a)$$

$$\frac{f_{l,n_{\max}+1}}{f_{l,n_{\max}}} \approx \frac{2(n_{\max}+l)+3}{2(n_{\max}+l)+1} \frac{\omega_{n_{\max}+l}}{\omega_{n_{\max}+l-1}} \times \frac{1 - \frac{2(n_{\max}+l)-1}{2(n_{\max}+l)+3} \frac{\omega_{n_{\max}+l+1}}{\omega_{n_{\max}+l}}}{1 - \frac{2(n_{\max}+l)-3}{2(n_{\max}+l)+1} \frac{\omega_{n_{\max}+l}}{\omega_{n_{\max}+l-1}}} \quad (11b)$$

$$\forall l \geq 1$$

Notice that in the relativistic regime  $\frac{q}{\epsilon} \rightarrow 1$  and all higher velocity weight integrals approach one another: We recover the usual hierarchy of equations for radiation. One can then set the (say adiabatic) initial conditions for the  $n = 0$  fluid properties as usual [23]

$$\delta = -2\psi \quad (12a)$$

$$\theta = \frac{1}{2}(k^2\tau)\psi \quad (12b)$$

$$\sigma = \frac{1}{15}(k\tau)^2\psi \quad (12c)$$

$$f_{l,0} = 0 \quad \forall l > 2 \quad (12d)$$

and since a ncdm component is relativistic early on, use  $f_{l,n} = f_{l,0} \quad \forall n > 0$  to set the initial condition for the remaining higher velocity weight fluid properties.

In the nonrelativistic regime, these variables get suppressed by powers of  $(q/\epsilon)^2 = v_\nu^2 \sim (T_\nu/m_\nu)^2$ , and similarly  $n = 0$  should suffice for most applications. During the transition, however, higher order contributions become important, and must be included for an accurate computation of the ncdm transfer functions. Only the case  $n_{\max} = 0$  was discussed in the literature thus far (see [25], and references therein).

In the traditional approach for including massive neutrinos in the computation of cosmological observables in linear theory, Eq.(7) are solved for a given number  $N_q$  of momentum bins, and up to some  $l_{\max}$ , i.e. a system of dimensionality  $N_q \times (l_{\max} + 1)$ . The solution is then used to perform the integrals in Eq.(5). The GBH is simpler in that it removes the extra step of performing the approximate momentum integrals, after solving the dynamical equations. However, it could be the case that the dimensionality of the GBH, i.e.  $(l_{\max} + 1) \times (n_{\max} + 1)$  is significantly bigger than  $N_q \times (l_{\max} + 1)$  (and it is actually what happens on the small scales), for the same achieved accuracy. Notwithstanding, in some cases a very large number of momentum bins is actually necessary, e.g. to

accurately obtain the effective sound speed [26]. The GBH is not plagued with the same issue since all momentum dependence is integrated out of the dynamical equations.

We now have everything we need, i.e. a closed system of dynamical equations plus suitable initial conditions, to consider the numerical implementation of the GBH. This will allow us to compare it with the Boltzmann solver CLASS.

## II. NUMERICAL IMPLEMENTATION

As an example of the numerical implementation of the GBH, we will consider an individual neutrino component with mass  $m_\nu = 0.1\text{eV}$ , at the intermediate scale of  $k = 0.01\text{Mpc}^{-1}$ . The mass is consistent with constraints from neutrino oscillations and cosmological data. Also, on the large scales (where neutrino velocities are unimportant) a simple viscous fluid approximation suffices i.e.  $l_{\text{max}} = 2, n_{\text{max}} = 0$  should be enough, while in small scales accurately obtaining the neutrino transfer functions is not so important because of free-streaming: Perturbations get washed-out and have a negligible impact on matter perturbations. Non-linear effects also start to kick-in.

The neutrino density contrast transfer function obtained from the GBH is compared to the output from CLASS. Boltzmann solvers do not produce accurate neutrino transfer functions at their default precision settings, as the codes are tailored to accurately produce the matter power spectrum, and relic neutrinos only have a subleading impact on this observable. To obtain accurate results, we follow the improved settings found in the appendix B of [26]: Turn off the CLASS  $\text{ncdm}$  fluid approximation, use a quadrature strategy to perform the  $q$ -integrals, with  $N_q = 30$  momentum bins, and set  $l_{\text{max}} = 30$ , i.e. a system of 930 equations. We then expect to get per mille accuracy for all redshifts, and for all scales of interest.

For simplicity, to evolve the GBH we use the sources  $\phi, \psi$  as given by CLASS. The initial conditions are set, according to Eq.(12), at some arbitrary early time, when all modes of interest are in super-horizon scales. We find that convergence, with respect to both  $l$  and  $n$  expansions, is roughly achieved for  $l_{\text{max}} = 10$  and  $n_{\text{max}} = 30$ , i.e. a system of 341 equations. The relative difference in the transfer functions generated from CLASS and the GBH can be found in Figure 1: There is per mille agreement for all values of redshift, so the GBH is accurately producing the neutrino transfer function.

For  $k = 0.03\text{Mpc}^{-1}$ , it was necessary to set  $l_{\text{max}} = 20$  and  $n_{\text{max}} \approx 250$ , corresponding to a much larger system of  $\approx 4500$  equations, to obtain sub-percent level agreement with CLASS. This shows that the  $n$  expansion is converging rather slowly on the small scales, so to solve the GBH on even smaller scales requires a more efficient numerical implementation. It might also be the case that a new truncation scheme can be found that alleviates

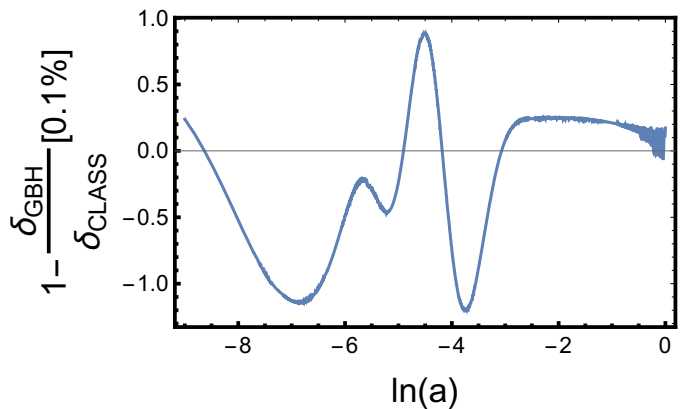


FIG. 1. Relative difference in the density contrast neutrino transfer function from the GBH and CLASS, in high precision settings, for a neutrino mass of  $m_\nu = 0.1\text{eV}$  and scale  $k = 0.01\text{Mpc}^{-1}$ . The GBH is truncated at  $l_{\text{max}} = 10$  and  $n_{\text{max}} = 30$ . The agreement is in the per mille level for all values of redshift. We conclude that the GBH is accurately producing the neutrino transfer functions. The transition from relativistic to non-relativistic regimes,  $a_{\text{tr}} \sim T_0/m_\nu$ , happens at around  $\ln(a_{\text{tr}}) \approx -5$ .

this issue (see the discussion in appendix A). Notwithstanding, and as pointed out before, on the small scales neutrinos free-stream, so it no longer becomes important that neutrino transfer functions are obtained very accurately (non-linearities also start to kick-in). In fact, we find that when switching to a viscous fluid approximation (FA) once the mode is sufficiently inside the horizon, the GBH produces the neutrino density contrast transfer function as accurately as CLASS in its default precision settings (where a similar switch to a viscous fluid approximation is also employed), over all scales of interest. This is illustrated in Figure 2.

As explained in the appendix A, both the  $l$  and  $n$  expansions are controlled by the parameter  $x = kT$ , with  $T$  the neutrino horizon (average comoving distance travelled by neutrino particles through cosmic history, see Eq.(A6) and comments below Eq.(A12), along with the plot in Figure 3). Specifically, if one wishes to follow the neutrino transfer function up to a time  $x$ , it seems to be the case that  $l_{\text{max}} \approx x/3$  is sufficient for convergence. The significant difference between  $T$  and  $\tau$  in the non-relativistic regimes, seen in Figure 3, now explains why one needs a much higher  $l_{\text{max}}$  for radiation than for massive neutrinos [23]. Similar cannot be said, unfortunately, about the  $n$  expansion, with a very slow convergence on the small scales. A more efficient numerical implementation is then necessary to (approximately) determine  $n_{\text{max}}$ , and hence the dimensionality of the system, as a function of  $x_{\text{max}}$ , which would allow us to arrive at a prescription to determine both  $n_{\text{max}}$  and  $l_{\text{max}}$  as a function of  $x_{\text{max}} = kT_{\text{max}}$ , and hence as a function of scale. Furthermore, a non-trivial  $n$  expansion was observed in the range of scales we probed: The error in the GBH, when compared to CLASS in high precision set-

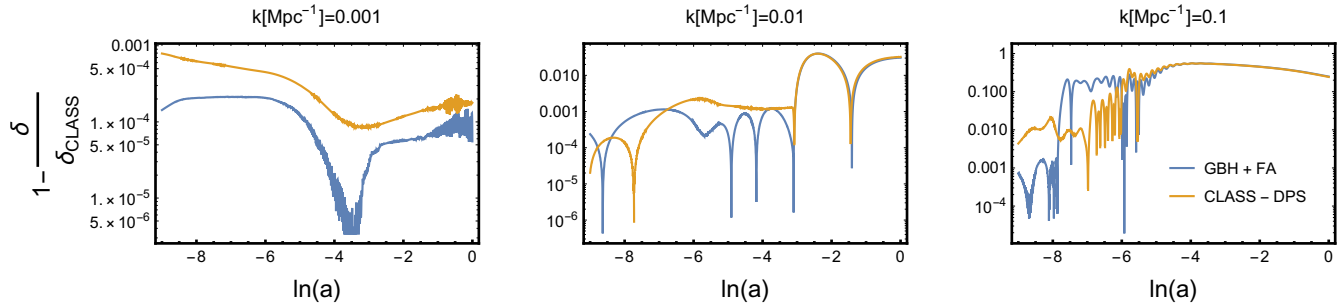


FIG. 2. Relative difference in the density contrast neutrino transfer function from the GBH, switching to a fluid approximation at  $x_{\max} = kT_{\max} = 15$  (GBH + FA) and CLASS in its default precision setting (CLASS-DPS), when compared to CLASS in high precision settings, for a neutrino mass of  $m_\nu = 0.1\text{eV}$ . The GBH is again truncated at  $l_{\max} = 10$  and  $n_{\max} = 30$ . Notice the agreement between methods when both are already in the FA regime, and hence solving the same dynamical equations. In its DPS, CLASS solves the Boltzmann hierarchy up to  $l_{\max} = 16$ , with  $N_q = 8$  momentum bins, and switches to the FA at  $k\tau_{\max} = 30$ .

tings, increased with  $n_{\max}$  for  $n_{\max} \sim O(1)$ , reaching a global maximum above which the error starts to decrease with increasing  $n_{\max}$ , eventually approaching zero. It would be interesting to determine if the same pattern is obtained for sub-horizon modes.

Finally, as derived in the appendix A,  $T \sim \sqrt{\frac{T_0}{m_\nu}}$  in the non-relativistic regime. It implies that, and for a given fixed scale  $k$ , one needs higher  $l_{\max}$  and  $n_{\max}$  for smaller neutrino masses (assuming that  $m_\nu$  is big enough for the transition to the non-relativistic regime to happen before today).

### III. CONCLUSION

We introduced the so-called generalized Boltzmann hierarchy (GBH) for non-cold dark matter (or ncdm) cosmological perturbations in a flat universe, a simpler alternative to the usual Boltzmann hierarchy for accurately producing neutrino transfer functions in the linear regime. It was determined that the GBH agrees with the Boltzmann solver CLASS, in its high precision settings, to a per mille level accuracy, in both large and intermediate scales compared to the neutrino free-streaming scale. Also, the GBH is as accurate as CLASS in its default precision settings, when switching to a viscous fluid approximation once a given mode enters the horizon.

As explained in the appendix A, on the small scales one needs to choose a very high  $n_{\max}$  in order to produce accurate neutrino transfer functions, and the numerical integration of the GBH becomes computationally very expensive. However, one should keep in mind that on small scales free-streaming effects, and non-linearities, start to kick-in, and hence the less important it becomes that the neutrino transfer functions are produced very accurately. For a given scale and accuracy goal, the GBH approach involves solving at least roughly the same num-

ber of equations as a standard Boltzmann solver would, but completely avoids the inconvenience, and computational challenges, associated to solving the hierarchy to later integrate over momentum space. Future work is needed to determine what exactly is the computational cost of the GBH, when compared to standard Boltzmann solvers, and its practical applicability for reproducing the dynamics of sub-horizon modes, i.e. without switching to the usual viscous fluid approximation.

We also compared the truncation scheme for the GBH with the one used in CLASS [25], in the case of  $l_{\max} = 2$  and  $n_{\max} = 0$ , i.e. a simple viscous fluid approximation. It was found that both truncation schemes are very similar, with the one from CLASS being tuned to produce slightly better results at late times, even though all individual approximations made in both schemes are of similar accuracy.

Overall, the GBH is a powerful tool to produce accurate neutrino transfer functions in linear theory, with integration being simpler and potentially faster than standard methods.

### ACKNOWLEDGMENTS

I am grateful to Marilena Loverde for helpful correspondence, guidance, and making comments on the drafts. I would also like to thank Julien Lesgourgues for the really nice and valuable comments on the final draft.

### Appendix A: Truncation scheme

We now look for a well-defined truncation scheme for the GBH: For a given neutrino mass  $m_\nu$  and scale  $k$ , we must be able to find values of  $l_{\max}$  and  $n_{\max}$  for which

the GBH accurately produces the neutrino transfer functions, and becomes insensitive to a further increase in these parameters. This is, of course, just the statement of convergence. From our experience with the Boltzmann hierarchy, we expect that convergence with respect to  $l_{\max}$  is not hard to achieve. In fact, we found that the following truncation, suggested in [23],

$$\Psi_{l_{\max}+1} \approx \frac{(2l_{\max}+1)\epsilon}{k\tau} \Psi_{l_{\max}} - \Psi_{l_{\max}-1} \quad (\text{A1})$$

is compatible with the structure of the GBH, and produces good results. Substitution of Eq.(A1) into Eq.(6) yields

$$f_{l_{\max}+1,n} \approx (l_{\max}+1) \left( \frac{1}{k\tau} f_{l_{\max},n} - \frac{l_{\max}}{4l_{\max}^2-1} f_{l_{\max}-1,n+1} \right) \quad (\text{A2})$$

for  $l_{\max} > 1$ . Next we move on to the truncation with respect to  $n_{\max}$ . First notice that

$$f_{l,n_{\max}+1} - f_{l,n_{\max}} \sim \int_0^\infty dq q^2 f_0(q) \epsilon \left( \frac{q}{\epsilon} \right)^{2n_{\max}+l} \times \left[ 1 - \left( \frac{q}{\epsilon} \right)^2 \right] \Psi_l \quad (\text{A3})$$

This integrand contains a term with the form  $f(y) = y^k(1-y^2)$ , for  $y \rightarrow q/\epsilon$ . This goes to zero in both the relativistic and non-relativistic regimes, with a peak in between that goes as  $1/k$  for  $k \gg 1$ . If our truncation scheme is based on finding an approximate expression for Eq.(A3), it seems reasonable to assume that convergence will be achieved for high enough  $n_{\max}$ . We proceed in analogy to what is done in [25]: Find an approximate expression to

$$\Lambda_0 := \frac{\delta_{n_{\max}+1}}{\delta_{n_{\max}}} = \frac{\int_0^\infty dq q^2 f_0(q) \epsilon \left( \frac{q}{\epsilon} \right)^{2n_{\max}+2} \Psi_0}{\int_0^\infty dq q^2 f_0(q) \epsilon \left( \frac{q}{\epsilon} \right)^{2n_{\max}} \Psi_0} \quad (\text{A4a})$$

$$\Lambda_l := \frac{f_{l,n_{\max}+1}}{f_{l,n_{\max}}} = \frac{\int_0^\infty dq q^2 f_0(q) \epsilon \left( \frac{q}{\epsilon} \right)^{2n_{\max}+l+2} \Psi_l}{\int_0^\infty dq q^2 f_0(q) \epsilon \left( \frac{q}{\epsilon} \right)^{2n_{\max}+l} \Psi_l} \quad (\text{A4b})$$

$$\forall l \geq 1$$

based on an educated guess on the  $q/\epsilon$  dependence of the multipoles  $\Psi_l$ . In order to investigate this carefully, let us go back to the Boltzmann hierarchy in Eq.(7). After setting

$$\Psi_l = -\frac{d \ln f_0}{d \ln q} \tilde{\Psi}_l \quad (\text{A5})$$

and introducing a new (q-dependent) time variable

$$\text{T} := \int_i \frac{d\tau}{\epsilon} \quad (\text{A6})$$

along with  $x = k\text{T}$ , the Boltzmann hierarchy reads

$$\frac{d\tilde{\Psi}_0}{dx} = -\tilde{\Psi}_1 + \frac{d\phi}{dx} \quad (\text{A7a})$$

$$\frac{d\tilde{\Psi}_1}{dx} = \frac{1}{3}(\tilde{\Psi}_0 - 2\tilde{\Psi}_2) + \frac{1}{3}\tilde{\psi} \quad (\text{A7b})$$

$$\frac{d\tilde{\Psi}_l}{dx} = \frac{1}{2l+1} [l\tilde{\Psi}_{l-1} - (l+1)\tilde{\Psi}_{l+1}] \quad (\text{A7c})$$

This is the same set of equations one would find for radiation, but in terms of the time parameter  $\text{T}$ , and a (q-dependent) effective gravitational potential  $\tilde{\psi} = (\epsilon/q)^2 \psi$ . This has two important consequences: First, all dependence on scales is actually encoded in  $x = k\text{T}$ , i.e. horizon crossing is effectively defined by the condition that  $k\text{T} \sim 1$ . Second, the mass dependence is encoded in  $x$ , but also in the effective gravitational potential, and in the non-relativistic limit it dominates the right-hand side of the evolution equation for  $\tilde{\Psi}_1$ : This is just the well-known decoupling of  $l < 2$  from higher multipoles in the non-relativistic regime. It is then true that

$$\tilde{\Psi}_1 \sim \int dx \tilde{\psi} \sim \int d\tau \frac{\epsilon}{q} \psi \quad (\text{A8})$$

and hence  $\tilde{\Psi}_1 \propto \epsilon/q$  to leading order, where we think of expanding  $\tilde{\Psi}_l$  in a power series on  $q/\epsilon$  around the non-relativistic regime. Substitution of this into Eq.(A7) now implies that  $\tilde{\Psi}_0 \propto 1$  and  $\tilde{\Psi}_l \propto (q/\epsilon)^{l-2}$  for  $l \geq 1$ , to leading order. This, combined with Eq.(A5), are used on Eq.(A4)

$$\Lambda_0 \approx \frac{\int_0^\infty dq q^2 f_0(q) \epsilon \frac{d \ln f_0}{d \ln q} \left( \frac{q}{\epsilon} \right)^{2(n_{\max}+1)}}{\int_0^\infty dq q^2 f_0(q) \epsilon \frac{d \ln f_0}{d \ln q} \left( \frac{q}{\epsilon} \right)^{2n_{\max}}} \quad (\text{A9a})$$

$$\Lambda_l \approx \frac{\int_0^\infty dq q^2 f_0(q) \epsilon \frac{d \ln f_0}{d \ln q} \left( \frac{q}{\epsilon} \right)^{2(n_{\max}+l)}}{\int_0^\infty dq q^2 f_0(q) \epsilon \frac{d \ln f_0}{d \ln q} \left( \frac{q}{\epsilon} \right)^{2(n_{\max}+l-1)}} \quad l \geq 1 \quad (\text{A9b})$$

After integration by parts, this can be written solely in terms of the background pressures  $P_n$  (or equation of state parameters  $\omega_n$ ) as follows:

$$\Lambda_0 \approx \frac{2n_{\max} + 5}{2n_{\max} + 3} \frac{\omega_{n_{\max}+1}}{\omega_{n_{\max}}} \frac{1 - \frac{2n_{\max}+1}{2n_{\max}+5} \frac{\omega_{n_{\max}+2}}{\omega_{n_{\max}+1}}}{1 - \frac{2n_{\max}-1}{2n_{\max}+3} \frac{\omega_{n_{\max}+1}}{\omega_{n_{\max}}}} \quad (\text{A10a})$$

$$\Lambda_l \approx \frac{2(n_{\max}+l)+3}{2(n_{\max}+l)+1} \frac{\omega_{n_{\max}+l}}{\omega_{n_{\max}+l-1}} \times \frac{1 - \frac{2(n_{\max}+l)-1}{2(n_{\max}+l)+3} \frac{\omega_{n_{\max}+l+1}}{\omega_{n_{\max}+l}}}{1 - \frac{2(n_{\max}+l)-3}{2(n_{\max}+l)+1} \frac{\omega_{n_{\max}+l}}{\omega_{n_{\max}+l-1}}} \quad (\text{A10b})$$

There is only one final piece of information that needs to be specified in order to complete the truncation scheme: How to choose the values of  $l_{\max}$  and  $n_{\max}$ . We know that higher multipoles and higher velocity weight

fluid properties contribute as small scale effects, acting as viscosity, since on large scales a simple fluid approximation suffices. Based on this, and the observations made following Eq.(A7), we expect that higher values of  $l_{\max}$  and  $n_{\max}$  are needed as  $x = kT$  increases.

Due to its importance, let us stop for a moment to study the time variable  $T$ , defined in Eq.(A6). During the relativistic regime, it is identical to  $\tau$ . Let us now see what happens in the non-relativistic regime, assuming that the time of transition  $a_{\text{tr}} \sim q/m_\nu$ , happens during matter domination, as is the case for massive neutrinos. We may then write the following approximation

$$T \approx \tau_{\text{tr}} + \int_{\text{tr}} \frac{da}{a} \frac{1}{aH} \frac{q}{m_\nu a} \quad (\text{A11})$$

where we split the integral from the initial time to the transition, and from the transition to the final time, use  $d\tau = \frac{da}{a} \frac{1}{aH}$ , with  $H = \frac{\dot{a}}{a}$  is the Hubble rate, and approximate  $\epsilon \approx m_\nu a$  in the non-relativistic regime, along with  $\epsilon \approx q$  up to the transition. Further using  $H \sim a^{-3/2}$  during matter domination, one obtains for the integral in the right-hand side of Eq.(A11)

$$\int_{\text{tr}} \frac{da}{a} \frac{1}{aH} \frac{q}{m_\nu a} \sim \frac{q}{m_\nu} \int_{\text{tr}} \frac{da}{a} a^{-\frac{1}{2}} \sim \frac{q}{m_\nu} a_{\text{tr}}^{-\frac{1}{2}} \sim \sqrt{\frac{q}{m_\nu}} \quad (\text{A12})$$

where we use the fact that the integral is dominated by its lower limit, and use  $a_{\text{tr}} \sim q/m_\nu$ . Further notice that during matter domination  $\tau_{\text{tr}} \sim a_{\text{tr}}^{1/2} \sim \sqrt{\frac{q}{m_\nu}}$  as well, so  $T \sim \sqrt{\frac{T_0}{m_\nu}}$  approaches a time-independent constant, as opposed to  $\tau$ , which grows indefinitely. In other words,  $T$  grows like  $\tau$  up to the time of transition, effectively freezing as one approaches the non-relativistic regime. We plot  $T$ , for  $q/T_0 = 3$  and  $m_\nu = 0.1\text{eV}$ , in Figure 3.

Indeed, since  $q/\epsilon = \nu_\nu$ ,  $T$  is the comoving distance travelled by a neutrino particle through cosmic history. When evaluated at the peak of the Fermi-Dirac distribution (say  $q/T_0 = 3$ ), this is roughly the neutrino horizon, or the free-streaming scale (integrated over e-folds). From this point forward, when used as a time variable, it is implicitly assumed that  $T$  is evaluated at  $q/T_0 = 3$ , and hence corresponds to the neutrino horizon.

On the large scales, i.e.  $x = kT \lesssim 1$ , a simple viscous fluid approximation with  $l_{\max} = 2$  and  $n_{\max} = 0$  suffices, and we discuss this in details in the appendix B. As  $x \gg 1$ , we expect that higher values of both  $l_{\max}$  and  $n_{\max}$  are needed. A reasonable assumption would then be that  $l_{\max}, n_{\max} \propto x$ . Indeed, our experience with the GBH seems to indicate that it converges for  $l_{\max} \approx x/3$ , with the difference between  $T$  and  $\tau$  explaining why one needs a much higher  $l_{\max}$  for radiation than for massive neutrinos [23]. Unfortunately, the same cannot be said about the  $n$  expansion, with  $n_{\max}$ , and hence the dimensionality of the system, growing very rapidly for modes inside the horizon. It is true that the  $q/\epsilon$  dependence of the multipoles deviate from their leading order expression we used for modes deep inside the horizon. It is

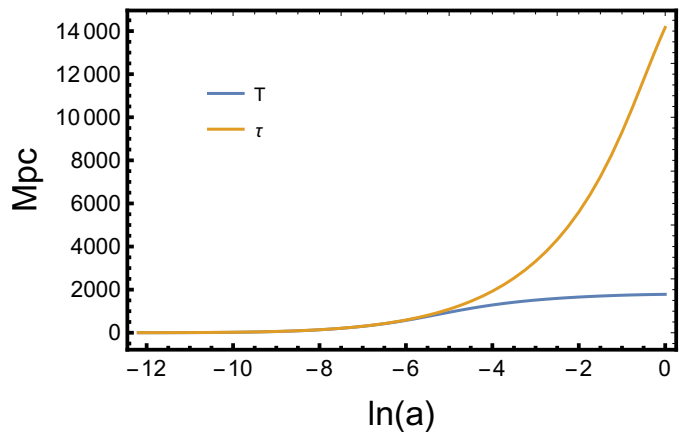


FIG. 3. Evolution of the neutrino horizon, i.e.  $T$  for  $q/T_0 = 3$ , and  $m_\nu = 0.1\text{eV}$ . It grows like  $\tau$  up to the time of transition, when it effectively freezes as it approaches the non-relativistic regime.

then plausible that a careful study of their actual  $q/\epsilon$  dependence, in this regime, could produce an improved truncation scheme that can help alleviate this issue of slow convergence.

## Appendix B: Fluid approximation

On large scales for which  $x = kT \lesssim 1$ , a simple viscous fluid approximation with  $l_{\max} = 2$  and  $n_{\max} = 0$  should suffice. Since in the non-relativistic regime  $T$  basically freezes at  $\tau_{\text{tr}}$ , the value of conformal time evaluated at the transition  $a_{\text{tr}} \sim \frac{q}{m_\nu} \sim \frac{T_0}{m_\nu}$ , this can be rephrased as to say that the mode has to be super-horizon at the transition, i.e. it enters the horizon during the non-relativistic regime. This is exactly what was found in [28], from comparing the exact solution with a simple fluid approximation.

Furthermore, on the small scales  $x \gg 1$ , free-streaming and non-linear effects start to kick-in and it no longer becomes important that the neutrino transfer function is produced very accurately. One can then choose a  $x_{\max}$  above which a simple fluid approximation can be used once again. Let us then stop for a moment to carefully study the case  $l_{\max} = 2$  and  $n_{\max} = 0$ . The fluid equations are given by Eq.(9). Our truncation scheme, developed in appendix A, provides approximations for the quantities  $\delta P/\delta\rho$ ,  $\Sigma$ ,  $\Theta$  and  $kf_3$ , in terms of the dynamical variables in the system.

Setting  $l_{\max} = 2$  and  $n_{\max} = 0$  in Eq.(A2) (which is known not to be a particularly good approximation for  $l_{\max} = 2$  [27]), one obtains

$$kf_3 \approx \frac{3}{\tau}\sigma - \frac{2}{5}\Theta \quad (\text{B1})$$

Both sides of this equation can be accurately determined at intermediate scales, from the GBH. A comparison can be found in Figure 4.



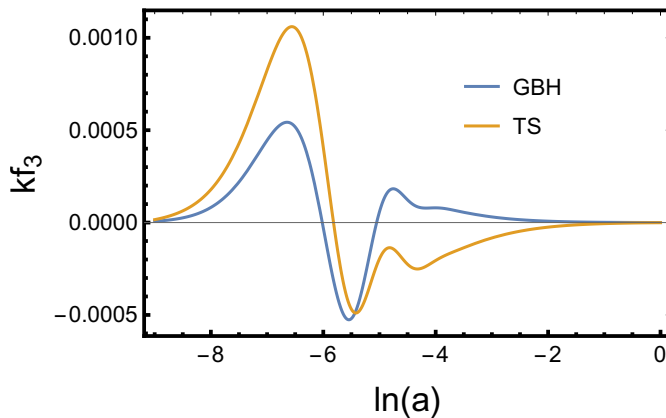


FIG. 4. Left (GBH) and right (TS) hand sides of Eq.(B1) as obtained from the GBH. Here  $k = 0.01\text{Mpc}^{-1}$ ,  $m_\nu = 0.1\text{eV}$ ,  $l_{\text{max}} = 10$  and  $n_{\text{max}} = 30$ . The approximation reproduces the right features, but is not accurate.

Furthermore, set  $n_{\text{max}} = 0$  into Eq.(A10) to arrive at

$$\frac{1}{3}\Lambda_0 = \frac{\delta P}{\delta\rho} \approx \frac{5}{3} \frac{\omega}{1+\omega} \left(1 - \frac{1}{5}\omega_2\right) = c_g^2 \quad (\text{B2a})$$

$$\Lambda_1 = \frac{\Theta}{\theta} \approx 3c_g^2 \iff c_{\text{vis}}^2 = \frac{3}{4}(1+\omega)c_g^2 \quad (\text{B2b})$$

$$\Lambda_2 = \frac{\Sigma}{\sigma} \approx \frac{7}{5} \frac{\omega_2}{\omega_1} \frac{1 - \frac{1}{7}\frac{\omega_3}{\omega_2}}{1 - \frac{1}{5}\frac{\omega_2}{\omega_1}} \quad (\text{B2c})$$

where a fluid viscosity speed  $c_{\text{vis}}$ , was introduced as a different parametrization to  $\Lambda_1$ , using notation from [29]

$$c_{\text{vis}}^2 = \frac{1}{4}(1+\omega)\frac{\Theta}{\theta} \quad (\text{B3})$$

In the CLASS ncdm fluid approximation, the truncation in the multipole is done in the exact same way as in Eq.(B1), while for the higher velocity weight quantities, the authors of [25] apply a bit of trial and error to arrive at the following ad-hoc approximations

$$\frac{1}{3}\Lambda_0 = \frac{\delta P}{\delta\rho} \approx \frac{5}{3} \frac{\omega}{1+\omega} \left(1 - \frac{1}{5}\omega_2\right) = c_g^2 \quad (\text{B4a})$$

$$\Lambda_1 = \frac{\Theta}{\theta} \approx 12 \frac{\omega}{1+\omega} c_g^2 \iff c_{\text{vis}}^2 = 3\omega c_g^2 \quad (\text{B4b})$$

$$\Lambda_2 = \frac{\Sigma}{\sigma} \approx \frac{\omega_2}{\omega_1} \quad (\text{B4c})$$

The Eqs.(B2) and (B4) differ slightly on the expressions for  $\Theta/\theta$  and  $\Sigma/\sigma$ .

In Figure 5 we compare the adiabatic sound speed squared to the exact solutions coming from both CLASS and the GBH: The GBH and CLASS agree in a per mille level, with both differing from the assumption of adiabaticity when approaching the non-relativistic regime.

In Figure 6, we compare the  $\Lambda_1$ 's from CLASS and GBH truncation schemes for the FA with the exact solution from the GBH: There is an overall 10% level error

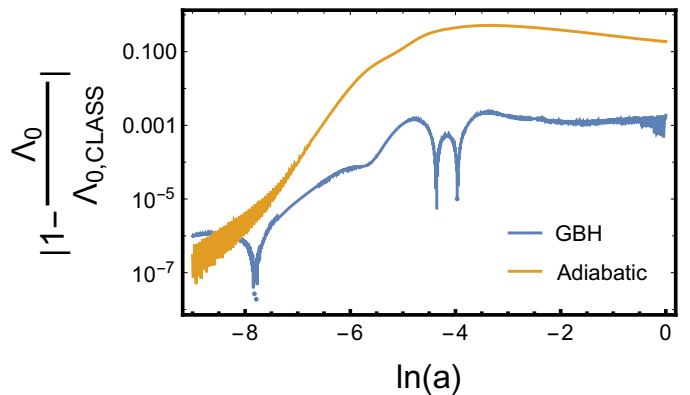


FIG. 5. Relative difference between sound speeds squared, coming from the GBH and the assumption of adiabaticity, when compared to the exact solution from CLASS. Here  $k = 0.01\text{Mpc}^{-1}$ ,  $m_\nu = 0.1\text{eV}$ ,  $l_{\text{max}} = 10$  and  $n_{\text{max}} = 30$ . The GBH and CLASS agree in a per mille level, with both differing from the assumption of adiabaticity when approaching the non-relativistic regime.

in both cases, but the GBH truncation scheme is an order of magnitude better in the non-relativistic regime. In Figure 7, we compare  $\Lambda_2$ 's from CLASS and GBH truncation schemes for the FA with the exact solution from the GBH: there is a 10% level error in both cases, and no significant difference between the two. Finally, in Figure 8 we compare fluid approximations, with GBH and CLASS truncation schemes, with the exact solution from CLASS: there is also an overall 10% level error in the neutrino density contrast transfer function, but the CLASS fluid approximation works slightly better at late times. Indeed, this is possible because the CLASS truncation scheme is tuned to produce the best outcome, even though all the individual approximations are in a similar level of accuracy as in the truncation scheme for the GBH, which was motivated from first principles. Because of this, the CLASS fluid approximation works better overall, and should be the one used in the regime  $x > x_{\text{max}}$ , as discussed.



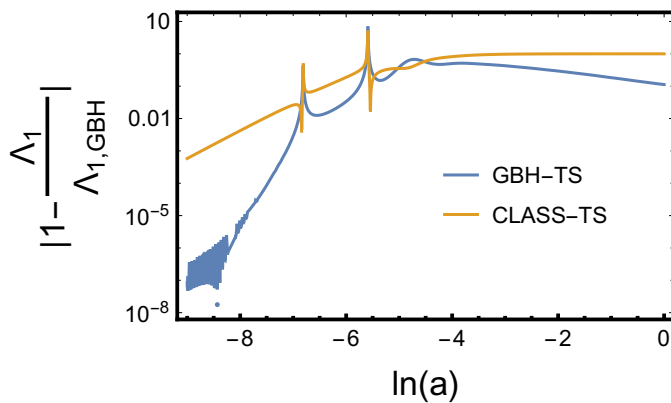


FIG. 6. Relative difference between  $\Lambda_1$ 's, coming from CLASS and GBH truncation schemes, when compared to the exact solution from the GBH. Here  $k = 0.01\text{Mpc}^{-1}$ ,  $m_\nu = 0.1\text{eV}$ ,  $l_{\text{max}} = 10$  and  $n_{\text{max}} = 30$ . There is an overall 10% level error in both cases, but the expression coming from the GBH truncation scheme is an order of magnitude better in the non-relativistic regime.

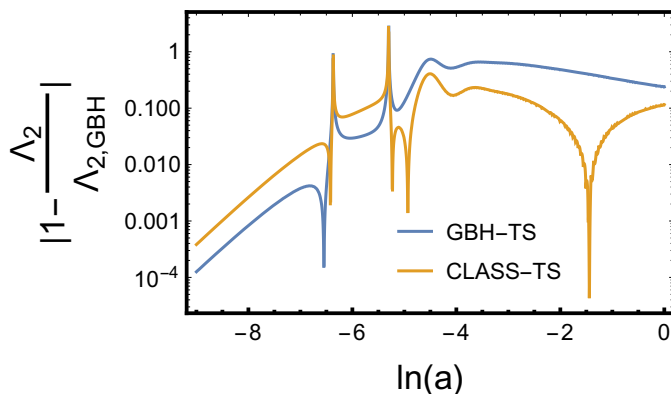


FIG. 7. Relative difference between  $\Lambda_2$ 's, coming from CLASS and GBH truncation schemes, when compared to the exact solution from the GBH. Here  $k = 0.01\text{Mpc}^{-1}$ ,  $m_\nu = 0.1\text{eV}$ ,  $l_{\text{max}} = 10$  and  $n_{\text{max}} = 30$ . There is an overall 10% level error in both cases, and no significant difference between the two.

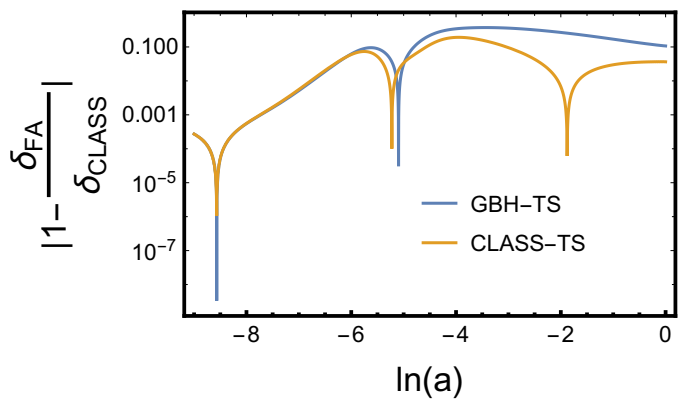


FIG. 8. Relative difference between neutrino transfer functions coming from the fluid approximation with GBH and CLASS truncation schemes, when compared to the exact solution from CLASS. Here  $k = 0.01\text{Mpc}^{-1}$ , and  $m_\nu = 0.1\text{eV}$ . There is an overall 10% level error in both cases, but the CLASS fluid approximation is tuned to yield slightly better results at late times.

- 
- [1] P. de Salas, D. Forero, C. Ternes, M. Tortola, and J. Valle, *Phys. Lett. B* **782**, 633 (2018), arXiv:1708.01186 [hep-ph].
- [2] P. De Salas, S. Gariazzo, O. Mena, C. Ternes, and M. Tórtola, *Front. Astron. Space Sci.* **5**, 36 (2018), arXiv:1806.11051 [hep-ph].
- [3] M. Gerbino, in *Prospects in Neutrino Physics* (2018) pp. 52–52, arXiv:1803.11545 [astro-ph.CO].
- [4] J. Lesgourgues and S. Pastor, *Phys. Rept.* **429**, 307 (2006), arXiv:astro-ph/0603494.
- [5] A. Loureiro *et al.*, *Phys. Rev. Lett.* **123**, 081301 (2019), arXiv:1811.02578 [astro-ph.CO].
- [6] N. Aghanim *et al.* (Planck), *Astron. Astrophys.* **641**, A6 (2020), arXiv:1807.06209 [astro-ph.CO].
- [7] S. W. Jha *et al.*, (2019), arXiv:1907.08945 [astro-ph.IM].
- [8] A. Blanchard *et al.* (Euclid), *Astron. Astrophys.* **642**, A191 (2020), arXiv:1910.09273 [astro-ph.CO].
- [9] N. Sehgal *et al.*, (2019), arXiv:1906.10134 [astro-ph.CO].
- [10] D. Spergel *et al.*, (2013), arXiv:1305.5422 [astro-ph.IM].
- [11] K. S. Dawson *et al.*, *Astron. J.* **151**, 44 (2016), arXiv:1508.04473 [astro-ph.CO].
- [12] L. Godfrey, H. Bignall, S. Tingay, L. Harvey-Smith, M. Kramer, S. Burke-Spolaor, J. Miller-Jones, M. Johnston-Hollitt, R. Ekers, and S. Gulyaev, *Publ. Astron. Soc. Austral.* **29**, 42 (2012), arXiv:1111.6398 [astro-ph.IM].
- [13] M. E. Levi *et al.* (DESI), (2019), arXiv:1907.10688 [astro-ph.IM].
- [14] C. Dvorkin *et al.*, (2019), arXiv:1903.03689 [astro-ph.CO].

- [15] T. Brinckmann, D. C. Hooper, M. Archidiacono, J. Lesgourgues, and T. Sprenger, *JCAP* **01**, 059 (2019), arXiv:1808.05955 [astro-ph.CO].
- [16] A. Slosar *et al.*, (2019), arXiv:1903.12016 [astro-ph.CO].
- [17] D. Green *et al.*, *Bull. Am. Astron. Soc.* **51**, 159 (2019), arXiv:1903.04763 [astro-ph.CO].
- [18] J. S. Bagla, *Curr. Sci.* **88**, 1088 (2005), arXiv:astro-ph/0411043.
- [19] V. Springel, *Mon. Not. Roy. Astron. Soc.* **364**, 1105 (2005), arXiv:astro-ph/0505010.
- [20] A. Lewis and A. Challinor, *ascl*, ascl (2011).
- [21] M. Zaldarriaga, U. Seljak, and E. Bertschinger, *Astrophys. J.* **494**, 491 (1998), arXiv:astro-ph/9704265.
- [22] J. Lesgourgues, (2011), arXiv:1104.2932 [astro-ph.IM].
- [23] C.-P. Ma and E. Bertschinger, *Astrophys. J.* **455**, 7 (1995), arXiv:astro-ph/9506072.
- [24] E. Bertschinger, *Phys. Rev. D* **74**, 063509 (2006), arXiv:astro-ph/0607319.
- [25] J. Lesgourgues and T. Tram, *JCAP* **09**, 032 (2011), arXiv:1104.2935 [astro-ph.CO].
- [26] J. Dakin, J. Brandbyge, S. Hannestad, T. Haugbølle, and T. Tram, *JCAP* **02**, 052 (2019), arXiv:1712.03944 [astro-ph.CO].
- [27] M. Archidiacono and S. Hannestad, *JCAP* **06**, 018 (2016), arXiv:1510.02907 [astro-ph.CO].
- [28] M. Shoji and E. Komatsu, *Phys. Rev. D* **81**, 123516 (2010), [Erratum: *Phys.Rev.D* 82, 089901 (2010)], arXiv:1003.0942 [astro-ph.CO].
- [29] W. Hu, *Astrophys. J.* **506**, 485 (1998), arXiv:astro-ph/9801234.